

## Mission Support for the Communications/Navigation Outage Forecast Satellite

DTIC COPY

D. L. Hysell

Cornell University  
Department of Earth and Atmospheric Sciences  
Ithaca, NY 14853

Scientific Report No. 3

30 August 2006

APPROVED FOR PUBLIC RELEASE; DISTRIBUTION UNLIMITED.



**AIR FORCE RESEARCH LABORATORY**  
**Space Vehicles Directorate**  
**29 Randolph Road**  
**AIR FORCE MATERIEL COMMAND**  
**Hanscom AFB, MA 01731-3010**

---

## NOTICES

Using Government drawings, specifications, or other data included in this document for any purpose other than Government procurement does not in any way obligate the U.S. Government. The fact that the Government formulated or supplied the drawings, specifications, or other data does not license the holder or any other person or corporation; or convey any rights or permission to manufacture, use, or sell any patented invention that may relate to them.

This report was cleared for public release and is available to the general public, including foreign nationals. Qualified requestors may obtain additional copies from the Defense Technical Information Center (DTIC) (<http://www.dtic.mil>). All others should apply to the National Technical Information Service.

AFRL-VS-HA-TR-2006-1118 HAS BEEN REVIEWED AND IS APPROVED FOR PUBLICATION IN ACCORDANCE WITH ASSIGNED DISTRIBUTION STATEMENT.

//Signature//

---

BAMANDAS BASU  
Contract Manager

//Signature//

---

JOEL MOZER, Chief  
Space Weather Center of Excellence

This report is published in the interest of scientific and technical information exchange, and its publication does not constitute the Government's approval or disapproval of its ideas or findings.

# REPORT DOCUMENTATION PAGE

Form Approved  
OMB No. 0704-0188

Public reporting burden for this collection of information is estimated to average 1 hour per response, including the time for reviewing instructions, searching existing data sources, gathering and maintaining the data needed, and completing and reviewing this collection of information. Send comments regarding this burden estimate or any other aspect of this collection of information, including suggestions for reducing this burden to Department of Defense, Washington Headquarters Services, Directorate for Information Operations and Reports (0704-0188), 1215 Jefferson Davis Highway, Suite 1204, Arlington, VA 22202-4302. Respondents should be aware that notwithstanding any other provision of law, no person shall be subject to any penalty for failing to comply with a collection of information if it does not display a currently valid OMB control number. PLEASE DO NOT RETURN YOUR FORM TO THE ABOVE ADDRESS.

<b>1. REPORT DATE (DD-MM-YYYY)</b> 30-08-2006		<b>2. REPORT TYPE</b> Scientific Report No. 3		<b>3. DATES COVERED (From - To)</b> Sep 2005 - Sep 2006	
<b>4. TITLE AND SUBTITLE</b> Mission Support for the Communication/Navigation Outage Forecast Satellite				<b>5a. CONTRACT NUMBER</b> F19628-03-C-0067	
				<b>5b. GRANT NUMBER</b>	
				<b>5c. PROGRAM ELEMENT NUMBER</b> 69120C	
<b>6. AUTHOR(S)</b> D. L. Hysell				<b>5d. PROJECT NUMBER</b> 1010	
				<b>5e. TASK NUMBER</b> CN	
				<b>5f. WORK UNIT NUMBER</b> A1	
<b>7. PERFORMING ORGANIZATION NAME(S) AND ADDRESS(ES)</b> Cornell University Department of Earth and Atmospheric Sciences Ithaca, NY 14853				<b>8. PERFORMING ORGANIZATION REPORT NUMBER</b>	
<b>9. SPONSORING / MONITORING AGENCY NAME(S) AND ADDRESS(ES)</b> Air Force Research Laboratory 29 Randolph Road Hanscom AFB, MA 01731-3010				<b>10. SPONSOR/MONITOR'S ACRONYM(S)</b> AFRL/VSBXP	
				<b>11. SPONSOR/MONITOR'S REPORT NUMBER(S)</b> AFRL-VS-HA-TR-2006-1118	
<b>12. DISTRIBUTION / AVAILABILITY STATEMENT</b> Approved for Public Release; Distribution Unlimited					
<b>13. SUPPLEMENTARY NOTES</b>					
<b>14. ABSTRACT</b> This is a project to provide mission support for the Communication/Navigation Outage Forecast System (C/NOFS) under BAA VS-03-01 during its first four years of operation. Cornell is required to support the mission with ground-based radar observations of background ionospheric parameters and of Equatorial Spread F (ESF) events from the Jicamarca Radio Observatory near Lima, Peru. In the pre-launch period for C/NOFS, Cornell and Jicamarca contributed to the project by measuring plasma density, drift, temperature, and composition profiles during eight campaign periods. Cornell's theoretical studies based on the radar observations of the postsunset bottomside F region have also identified a new plasma shear instability that acts as a seed for the observed large-scale density irregularities. In this report, the field-line averaged linear growth rate of the instability and its comparison with that of the generalized Rayleigh-Taylor instability are presented. The shear instability may be used as a tool for understanding and forecasting of ESF. The instability model and its forecasting capability will improve when C/NOFS measurements are available.					
<b>15. SUBJECT TERMS</b> Collisional Shear instability, Ionospheric Irregularities, Spread F, Jicamarca radar, Range-time-intensity (RTI)					
<b>16. SECURITY CLASSIFICATION OF:</b>			<b>17. LIMITATION OF ABSTRACT</b>  SAR	<b>18. NUMBER OF PAGES</b>  12	<b>19a. NAME OF RESPONSIBLE PERSON</b> Bamandas Basu
<b>a. REPORT</b> UNCLASSIFIED	<b>b. ABSTRACT</b> UNCLASSIFIED	<b>c. THIS PAGE</b> UNCLASSIFIED			<b>19b. TELEPHONE NUMBER (include area code)</b> 781-377-3048

## Contents

1 INTRODUCTION	4
2 METHODS AND PROCEDURES	4
3 BIBLIOGRAPHY	9

## List of Figures

1	Range time intensity (RTI) image depicting a patchy bottom-type layer prior to the onset of ESF. . . . .	5
2	Another RTI image showing a patchy bottom-type layer in advance of ESF irregularities. . . . .	5
3	Jicamarca ISR data from June. The four rows depict plasma density, electron temperature, ion temperature, and $H^+$ fraction. The $He^+$ fraction was not fit due to the low signal-to-noise ratio. . . . .	8

# 1 INTRODUCTION

This is a project to provide mission support for the Communication/Navigation Outage Forecast System (C/NOFS) under BAA VS-03-01 during its first four years of operation. Cornell will support the mission with ground-based radar observations of background ionospheric parameters and of equatorial spread  $F$  (ESF) events from the Jicamarca Radio Observatory near Lima, Peru. Jicamarca is capable of measuring ionospheric electric field and conductivity profiles from the valley region well into the topside ionosphere. Jicamarca can also make very detailed observations of ionospheric irregularities associated with ESF. Three main tasks will be supported under this project: (1) in-flight calibration of the electric field/drift meter sensors on board the spacecraft, (2) provision of Jicamarca radar support for experimental campaigns, both before the launch and during the satellite operations, and (3) analysis and interpretation of the data obtained during these campaigns in light of the C/NOFS mission goals.

# 2 METHODS AND PROCEDURES

The protracted pre-launch period for C/NOFS has afforded the opportunity to reexamine fundamental instability theory and rethink the mission forecast strategy. Emphasis now lies in using the theory developed by [2] regarding plasma shear instabilities in the postsunset bottomside  $F$  region ionosphere as a tool for understanding and forecasting equatorial spread  $F$ . The basic idea is that the shear instability is more robust than the ionospheric interchange instability immediately after sunset and that the former serves as a seed for the latter, which appears otherwise to grow too slowly to account for the rapid production of large-scale irregularities often observed. If so, then the parameters being measured and modeled by the C/NOFS science team should be modified accordingly. The changes required are not drastic, as the shear instability is closely related to the ionospheric interchange instability. Furthermore, proxies for shear instabilities should themselves be monitored. These include so-called bottom-type scattering layers, which are common features of the postsunset equatorial ionosphere and which are known to become patchy very early in the evolution of large-scale waves and irregularities.

Bottom-type layers represent a necessary condition for ESF. Patchy bottom-type layers more often appear to be a sufficient condition. These strong statements are based on long-term studies at Jicamarca and on results from the NASA EQUIS II rocket campaign on Kwajalein in the summer of 2004. Patchy layers have been observed at Jicamarca using radar imaging and on Kwajalein using the scanning Altair radar. Occasionally, the patchiness of the layers is apparent in conventional range-time-intensity (RTI) radar data from Jicamarca. Fig. 1 illustrates a broken layer exhibiting  $\sim 40$  min. periodicity telltale of a large-scale precursor wave with a wavelength of the order of 100–200 km. Fig. 1 shows another patchy bottom-type layer, this time with  $\sim 10$  min. periodicity indicative of a large-scale precursor wave with a wavelength of a few tens of kilometers. These two scale sizes are prevalent in imaging and Altair data.

Most often, however, RTI data from the JULIA radar at Jicamarca (which has been running semi-nightly for ten years) give no clear indication of whether bottom-type layers are patchy or continuous. Standard JULIA modes were designed for a synoptic view of  $E$  and  $F$  region irregularities and not explicitly to monitor bottom-type layers. We have therefore instituted a new JULIA radar mode which will be in operation during the remainder of the C/NOFS pre-launch period. The mode is optimized to detect irregular bottom-type layers using two approaches. One of these is a split-beam approach, whereby the echoes from two radar beams directed eastward and westward, respectively, will be compared. Significant differences in echo power will indicate

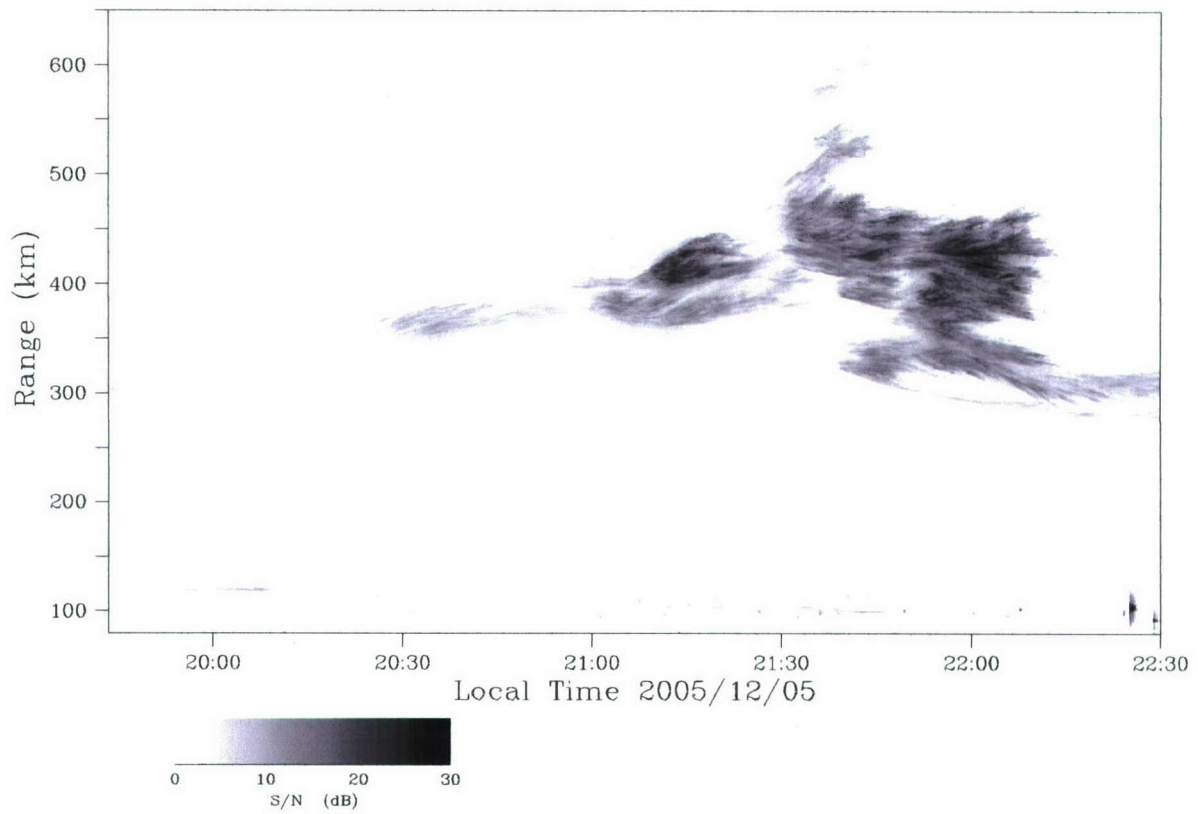


Figure 1: Range time intensity (RTI) image depicting a patchy bottom-type layer prior to the onset of ESF.

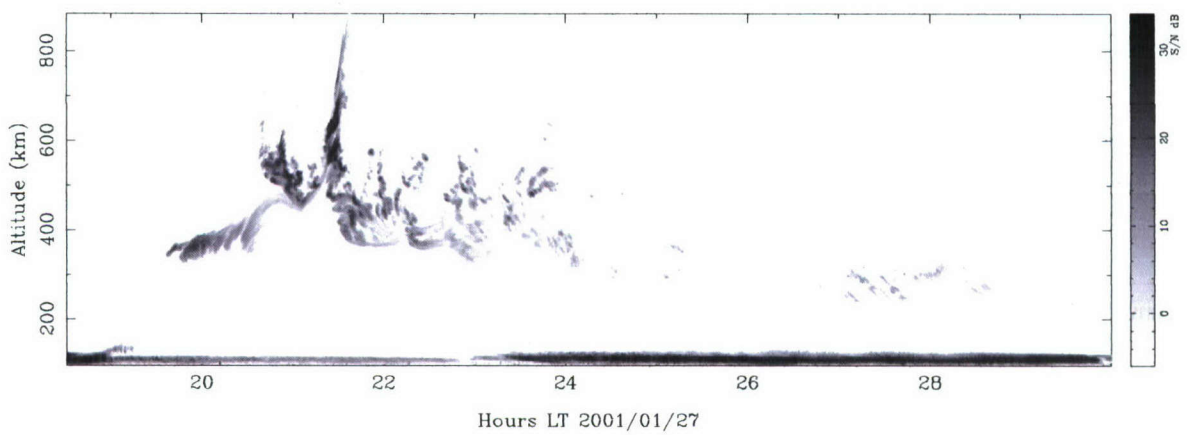


Figure 2: Another RTI image showing a patchy bottom-type layer in advance of ESF irregularities.

horizontal inhomogeneity at the scale size of the beam separation. The other approach involves interferometry. Echoes corresponding to one of the beams will be processed using spaced receiver correlation. The coherence of the signals will indicate horizontal inhomogeneity at the scale size of the radar beamwidth. An expert system will assess the data and eventually be applied to near real-time forecasting. Data collection using the new mode is underway.

The best prospect for advance spread  $F$  forecasting, however, involves anticipating ESF by estimating the growth of the underlying shear instability. We can do this by continuously evaluating the appropriate linear growth rate expression, much as the conventional strategy calls for evaluating the ionospheric interchange instability growth rate. A combination of experimental and model data will be required, and these must ultimately be available on an operational basis. The existing C/NOFS forecast strategy already incorporates these elements.

We recently derived the linear growth rate for the collisional shear instability. This is an inherently nonlocal instability, and the semi-local expression we found is at best an approximation. Exact results for a slab geometry have been obtained by [2]. Our expression has been validated against numerical models and simulations [3].

This calculation takes places in magnetic dipole coordinates  $(p, q, \Phi)$  described by [1]. The plasma number density and potential are separated into zero- and first-order components according to

$$\begin{aligned}\phi(p, q, \Phi) &= \phi_o(p) + \phi_1(p)e^{i(\kappa\phi - \omega t)} \\ n(p, q, \Phi) &= n_o(p) + n_1(p, q)e^{i(\kappa\phi - \omega t)}\end{aligned}$$

where  $\phi_o$  is the potential associated with the background zonal  $\mathbf{E} \times \mathbf{B}$  plasma drift ( $v_o(p)$ ), and  $n_o(p)$  expresses the background plasma density gradient.

To first order, the continuity equation can be written as:

$$(\omega - kv_o)n_1 + \frac{1}{h_p} \frac{dn_o}{dp} \frac{\kappa}{h_\phi} \frac{\phi_1}{B} = 0 \quad (1)$$

where  $h_\phi$  is the scale factor associated with the  $\Phi$  coordinate, for example, and  $B$  is the background magnetic field. The dominant first order plasma drift velocity is the  $\mathbf{E} \times \mathbf{B}$  drift arising from  $\phi_1$ .

We next invoke the quasineutrality condition,  $\nabla \cdot \mathbf{J} = 0$ . We evaluate the transverse component of the divergence of the current density, a quantity that vanishes when integrated along a magnetic field line between points where it exits the ionosphere. The primary first order currents we consider are Pedersen currents arising from  $\phi_1$  and from density perturbations  $n_1$  embedded in a background electric field, which in the frame of reference of the neutral gas moving with zonal speed  $u$  is proportional to  $u - v_o$ .

$$\begin{aligned}\frac{\partial}{\partial p} \left( \frac{h_\phi h_q}{h_p} \sigma_P \frac{\partial \phi_1}{\partial p} \right) - \frac{h_p h_q}{h_\phi} \sigma_P \kappa^2 \phi_1 \\ - \frac{\partial}{\partial p} \left( h_\phi h_q \sigma_P \frac{n_1}{n_o} (u - v_o) B \right) = \nabla_\perp \cdot \mathbf{J}\end{aligned} \quad (2)$$

where  $\sigma_P(p)$  is the Pedersen conductivity. Combining (1) and (2) gives:

$$\begin{aligned}\frac{\partial}{\partial p} \left( \frac{h_\phi h_q}{h_p} \sigma_P \frac{\partial \phi_1}{\partial p} \right) - \frac{h_p h_q}{h_\phi} \sigma_P \kappa^2 \phi_1 \\ + \frac{\partial}{\partial p} \left( \frac{h_q}{h_p} \sigma_P \frac{u - v_o}{\omega - (\kappa/h_\phi)v_o} \kappa \frac{1}{n_o} \frac{dn_o}{dp} \phi_1 \right) = \nabla_\perp \cdot \mathbf{J}\end{aligned}$$

The next step in the derivation is to multiply the preceding equation by  $\phi_1^*$  and integrate over a neighborhood of  $p$  where the perturbed potential is significant. In the formulas to follow, the  $p$  integration is not written but is understood. Applying integration by parts and dropping the boundary terms then yields:

$$-\frac{h_\phi h_q}{h_p} \sigma_P |\phi_1'|^2 - \frac{h_p h_q}{h_\phi} \sigma_P \kappa^2 |\phi_1|^2 - \frac{h_q}{h_p} \sigma_P \frac{u - v_o}{\omega - (\kappa/h_\phi)v_o} \kappa \frac{n_o'}{n_o} \phi_1 \phi_1'^* = \nabla_\perp \cdot \mathbf{J} \phi_1^*$$

where the prime superscript represent differentiation with respect to  $p$ .

At this point, we make two assumptions which are motivated by the exact solutions obtained computationally by [2]. The first is that the real part of the frequency of the growing wave is well approximated by the Doppler shift, i.e.  $\omega \approx (\kappa/h_\phi)v_o + i\gamma$ . The second is that in the vicinity of its peak, the perturbed potential varies approximately according to  $\exp(i\kappa_p p)$ . This is essentially a local approximation except that we remember to maintain the  $p$  integration described above in the analysis. To avoid confusion, we replace  $\kappa$  from above with  $\kappa_\phi$  in equations that follow.

At this point, we have

$$-\frac{h_\phi h_q}{h_p} \sigma_P \kappa_p^2 |\phi_1|^2 - \frac{h_p h_q}{h_\phi} \sigma_P \kappa_\phi^2 |\phi_1|^2 + \frac{h_q}{h_p} \sigma_P \frac{u - v_o}{\gamma} \kappa_p \kappa_\phi \frac{n_o'}{n_o} |\phi_1|^2 = \nabla_\perp \cdot \mathbf{J} \phi_1^* \quad (3)$$

Integrating (3) over magnetic field lines from end to end in the ionosphere and taking the potential to be invariant along the integral then produces the flux tube integrated growth rate estimate in (4), since  $\langle \nabla_\perp \cdot \mathbf{J} \rangle = J_\parallel|_{\text{endpoints}} = 0$ .

$$\gamma_{cs} \approx \frac{\kappa_\phi \kappa_p \langle \frac{h_q}{h_p} \sigma_P (u - v_o) n_o' / n_o \rangle}{\kappa_\phi^2 \langle \frac{h_p h_q}{h_\phi} \sigma_P \rangle + \kappa_p^2 \langle \frac{h_\phi h_q}{h_p} \sigma_P \rangle} \quad (4)$$

$$\gamma_{grt} \approx \frac{\langle \frac{h_q}{h_\phi} \sigma_P (E_o/B + g_\perp / \nu_{in}) n_o' / n_o \rangle}{\langle \frac{h_p h_q}{h_\phi} \sigma_P \rangle} \quad (5)$$

Note that the angle brackets in (4) imply an average over the span of  $p$  where the perturbed potential is significant in addition to an average over the field line. This span is likely to be quite narrow in the early stages of instability since small spans are associated with the largest growth rates. A similar (but simpler) approach yields the more exact growth rate estimate for the generalized Rayleigh Taylor instability in (5), which is a well-known result.

The growth rate estimates necessitate the specification of ionospheric Pedersen conductivities, winds, and electric fields over the magnetic flux tubes of interest. Jicamarca can measure plasma number densities and electric fields overhead, but models are necessary to complete the off-equatorial specification. Winds likewise require modeling, and we expect empirical models of the thermospheric winds to improve once C/NOFS wind measurements are available.

The estimates are no better than the models supporting them, and we have been collecting baseline data at Jicamarca in order to help validate the C/NOFS physics-based background model (and also to support the COSMIC mission). Data from the June campaign are shown in Fig. 3. The first day of observations were marred by technical problems, and overall data quality suffers

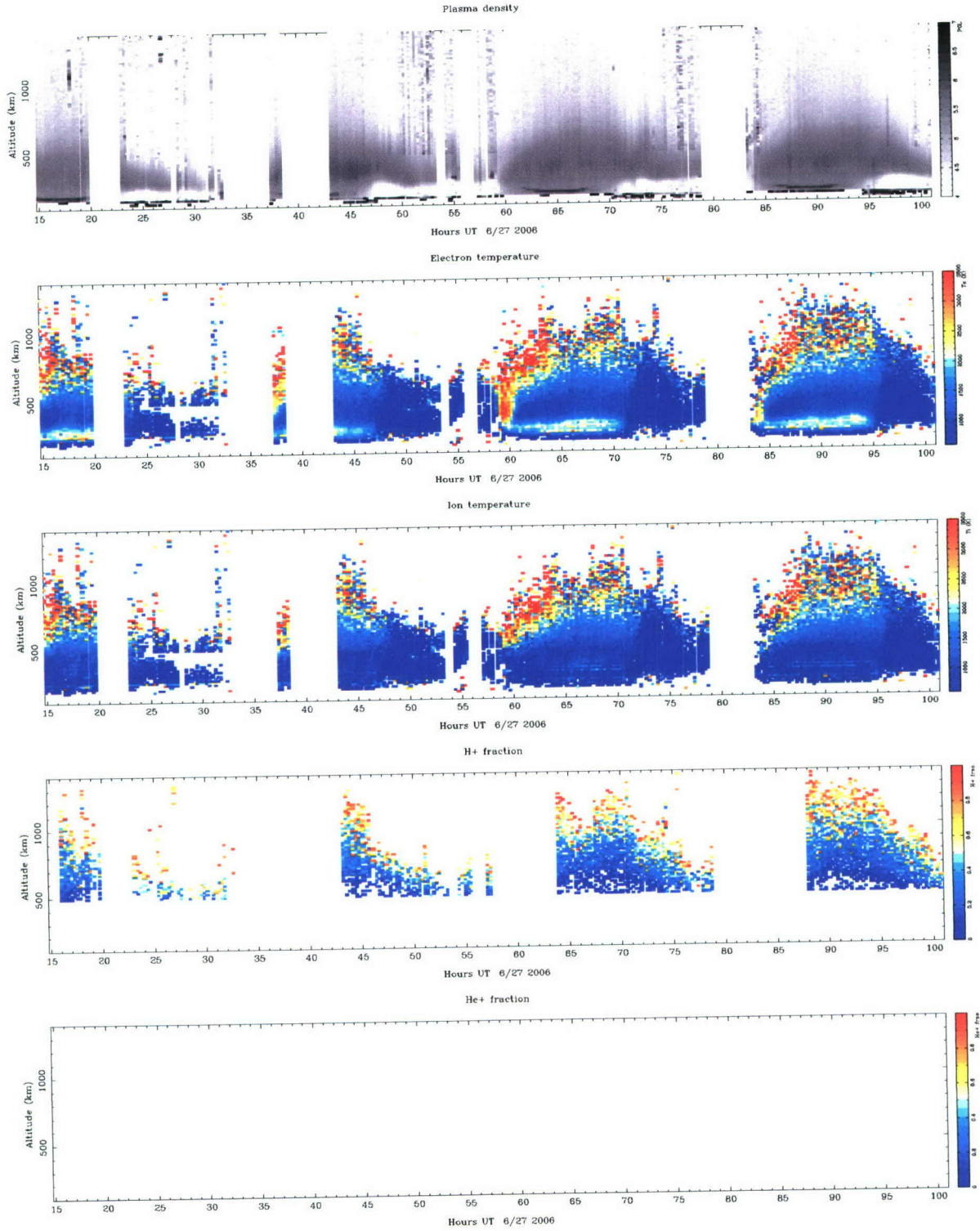


Figure 3: Jicamarca ISR data from June. The four rows depict plasma density, electron temperature, ion temperature, and H<sup>+</sup> fraction. The He<sup>+</sup> fraction was not fit due to the low signal-to-noise ratio.

from very low solar flux, ionospheric content, and signal levels. Nevertheless, the data highlight two crucial features of the equatorial ionosphere not well represented by existing empirical or physics-based models. These are 1) a very steep bottomside density gradient after sunset with a scale length of the order of 10 km and 2) a relatively dense postsunset valley region, with densities of nearly  $10^4 \text{ cm}^{-3}$ . The one model that seems to be able to reproduce these features accurately is the PIM model. This is no accident, as PIM has been tuned to reproduce the climatology observed at Jicamarca.

More C/NOFS/COSMIC validation campaigns are scheduled for the fall of 2006. There is little point in attempting to forecast ESF on the basis of the arguments presented here until contemporary physics-based models can be made reproduce data like those in Fig. 3 and those acquired during the EQUIS II campaign more accurately. We are working with our colleagues at AFRL and on the C/NOFS EWG to improve the situation.

### 3 BIBLIOGRAPHY

#### References

- [1] D. L. Hysell, J. Chun, and J. L. Chau. Bottom-type scattering layers and equatorial spread  $F$ . *Ann. Geophys.*, 22:4061, 2004.
- [2] D. L. Hysell and E. Kudeki. Collisional shear instability in the equatorial  $F$  region ionosphere. *J. Geophys. Res.*, 109:(A11301), 2004.
- [3] D. L. Hysell, E. Kudeki, and J. L. Chau. Possible ionospheric preconditioning by shear flow leading to equatorial spread  $F$ . *Ann. Geophys.*, 23:2647, 2005.